Influence of double occupancy and lattice distortions on the magnetic phase diagram of $A_{1-x}A'_xMnO_3$

Michel van Veenendaal and A. J. Fedro
Northern Illinois University, De Kalb, Illinois 60115
and Argonne National Laboratory, 9700 South Cass Avenue, Argonne, Illinois 60439
(Received 1 May 1998)

A model is presented that describes the competition between the ferromagnetic and several antiferromagnetic structures observed in the $A_{1-x}A'_xMnO_3$ series. It is found that the strong asymmetry of the magnetic phase diagram, i.e., predominantly ferromagnetic for $x<0.5$ and antiferromagnetic for $x>0.5$, can readily be explained by extending the double exchange model to include double occupancy. The strong charge fluctuations between different MnO_6 clusters are the result of the charge-transfer-like nature of the manganites. The dependence of the magnetic structure on lattice distortions is described. The appearance of different magnetic structures around $x=0.5$ is interpreted in terms of changes in the Mn-O-Mn bond angle and the Jahn-Teller distortions. [S0163-1829(99)05501-0]

Recently, there has been a renewed interest in the manganate perovskites $A_{1-x}A'_xMnO_3$, where A are trivalent rare-earth ions, such as, La, Nd, or Pr, and A' divalent cations, such as, Ba, Ca, or Sr. For $0.2<x<0.4$ these materials show strong magnetoresistive effects.[1] Theoretically the focus so far has been on the interplay between magnetic and transport properties. However, a number of other intriguing issues has been given little theoretical attention.

First, the phase diagram is predominantly ferromagnetic for $x<0.5$ and antiferromagnetic for $x>0.5$.[2,3] The standard double exchange model[4–6] and also related models,[7] however, generally predict roughly equal antiferromagnetic regions for x greater and less than 0.5. This can be understood by noting that holes in a background of $S=2$ spins (x close to zero) are expected to behave similarly to electrons in a background of $S=\frac{3}{2}$ spins (x close to one).

Secondly, recent experiments show a strong dependence of the magnetic properties on lattice distortions. For $x=0.3$, Hwang *et al.*[8] have found that a decrease of the Mn-O-Mn bond angle behaves similarly to a decrease in hole doping. Furthermore, for $x\sim0.5$, magnetic phase transitions are always accompanied by lattice deformations.[9,10]

We present here a model that provides an intuitive and semiquantitative interpretation of these phenomena. Usually the manganites are studied with an effective model where each site represents a MnO_6 cluster. The effective on-site interaction $U_{\rm eff}$ is often assumed to be of the order of the Coulomb interaction between the $3d$ electrons U_{dd}. Since $U_{dd}\cong5-6$ eV one often takes the limit $U_{\rm eff}\rightarrow\infty$. High-energy spectroscopy and, in particular, O $1s$ x-ray absorption spectroscopy,[11,12] however, provide strong evidence that the manganites are in the charge-transfer regime.[13] This implies that the relevant parameter for charge fluctuations is the charge-transfer energy, i.e., for $AMnO_3$, $U_{\rm eff}\cong\Delta_{e_g}=E(t_{2g}^3e_g^2\underline{L})-E(t_{2g}^3e_g)$, where $\underline{L}$ indicates a hole on the oxygen. For manganese oxides $\Delta_{e_g}\sim1-2$ eV, i.e., of the order of the insulating gap in $LaMnO_3$.

The next observation to make is on the different types of magnetic structures classified by Wollan and Koehler;[2] some of them are reproduced in Fig. 1. The ferromagnetic regions of these structures are stabilized by the gain in kinetic energy of the e_g electrons as a result of the alignment of the spins formed by the t_{2g} electrons. Anderson and Hasegawa[5] have shown that the effective hopping is proportional to $\cos(\theta/2)$, where θ is the angle between two neighboring t_{2g} spins. For classical spins this implies that the hybridization between antiferromagnetically coupled sites is zero. In this limit the e_g electrons hop in ferromagnetic regions of dimension 3, 2, 1, and 0 for the structures F, A, C, and G, respectively. Obviously, the gain in kinetic energy becomes smaller for lower dimensions. However, this can be compensated by the increase in the number of antiferromagnetic bonds from 0, 2, 4, to 6 per site for the F, A, C, and G structures, respec-

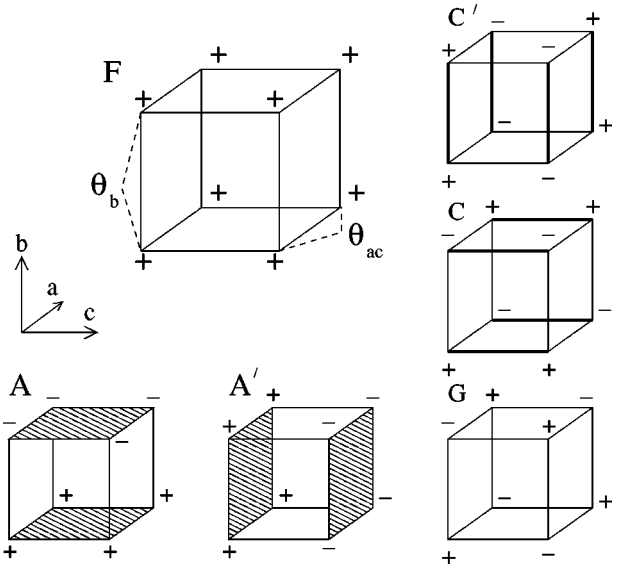

FIG. 1. Different magnetic structures found in the manganites. F, A, C, and G have ferromagnetic regions of dimensions 3, 2, 1, and 0, respectively. θ_{ac} and θ_b are the Mn-O-Mn bond angles in the ac plane and along the b axis, respectively. A' and C' are obtained by rotating A and C, respectively, by 90°. The + and − denote up and down core spins, respectively.

tively. Wollan and Koehler also identify a *CE* structure, which can be thought of as ferromagnetic chains that zigzag in the ac plane. We have omitted this structure since the stabilization energy should be similar to the *C* structure.

To describe the competition between the different magnetic structures we have studied the relative contributions of the kinetic energy of the e_g electrons in ferromagnetic regions of different dimensions and the superexchange of the t_{2g} electrons. We have included the effects of double occupancy and the twofold degeneracy of the e_g orbitals. Effective parameters are obtained by diagonalization of Mn-O-Mn clusters, taking into account the fact that the manganites are in the charge-transfer regime.

Since the Hund's coupling between the t_{2g} spins and the e_g electrons is of the order of 2 eV, the ferromagnetic regions are predominantly populated by e_g electrons with their spins parallel to that of the t_{2g} electrons. This effectively makes the itinerant electrons spinless fermions whose Hamiltonian is given by

$$H=\sum_{i,j,\alpha,\alpha'} t_{\mathrm{eff}}(i\alpha,j\alpha')c^{\dagger}_{i\alpha}c_{j\alpha'}+U_{\mathrm{eff}}\sum_{i} n_{i1}n_{i,-1}, \quad (1)$$

where α runs over the orbitals $1=x^2-y^2$ and $-1=3z^2-r^2$. This Hamiltonian is similar to the Hubbard model except that one has two different kinds of orbitals instead of up and down spins and the presence of cross terms between the two orbitals in the hopping term. In this Hamiltonian, the hopping is between effective sites, each representing a MnO_6 cluster. However, in the real system the hopping goes via the oxygen. The effective hopping parameter t_{eff} therefore depends on parameters such as the difference in orbital energies between oxygen and manganese and, as we will discuss in more detail below, the Mn-O-Mn bond angle. To account for these effects we calculate t_{eff} by considering a Mn-O-Mn cluster.[14] The basis set includes the Mn $3d$ orbitals and the O $2p$ orbitals. For this small cluster the model parameters are the difference in orbital energies of oxygen and manganese e_g orbital Δ_{e_g} and the hybridization matrix elements of the e_g orbitals and the σ-bonding oxygen orbitals given by $(pd\sigma)=0.5$ eV. The resulting many-body Hamiltonian is then diagonalized exactly. The effective hopping matrix elements $t_{\mathrm{eff}}(i\alpha,j\alpha')$ are derived from the bonding-antibonding splitting; the matrix elements follow the usual Slater-Koster relationships for d electrons.[15] U_{eff} is equal to $E(2)+E(0)-2E(1)$ where $E(n)$ is the lowest energy of a MnO_6 cluster with n e_g electrons. U_{dd} has been taken 5 eV.

We solve the Hamiltonian in Eq. (1) following the approach of Kotliar and Ruckenstein.[16] Four boson operators, that specify the occupation number of the empty (e_i), singly-occupied with an electron in orbital α ($p_{i\alpha}$), and doubly occupied (d_i) states at site i, are introduced. The unphysical states introduced by this enlarged basis set can be removed by introducing the on-site constraints

$$e_i^2+p_{i1}^2+p_{i,-1}^2+d_i^2=1 \quad (2)$$

and

$$p_{i\alpha}^2+d_i^2=n_{i\alpha}, \quad (3)$$

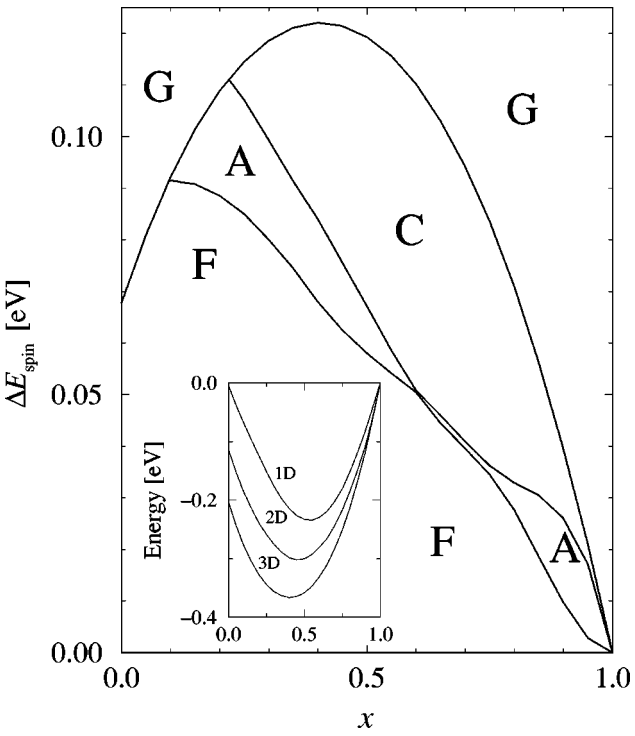

FIG. 2. The inset shows the total kinetic energy of the ferromagnetic regions as a function of x for one, two, and three dimensions. The phase diagram shows the magnetic structure with the lowest energy as a function of x versus the energy needed to turn two neighboring spins ΔE_{spin}.

where $n_{i\alpha}$ is the number of electrons on site i in the orbital with index α. The Hamiltonian now transforms into

$$\tilde{H}=\sum_{i,j,\alpha,\alpha'} t_{\mathrm{eff}}(i\alpha,j\alpha')\tilde{z}^{\dagger}_{i\alpha}\tilde{z}_{j\alpha'}c^{\dagger}_{i\alpha}c_{j\alpha'}+U_{\mathrm{eff}}\sum_{i} d_i^{\dagger}d_i. \quad (4)$$

The operators $\tilde{z}_{i\alpha}$,

$$\tilde{z}_{i\alpha}=(1-p^{\dagger}_{i\alpha}p_{i\alpha}-d_i^{\dagger}d_i)^{-1/2}(e_i^{\dagger}p_{i\alpha}+p^{\dagger}_{i,-\alpha}d_i)\times(1-p^{\dagger}_{i,-\alpha}p_{i,-\alpha}-e_i^{\dagger}e_i)^{-1/2}, \quad (5)$$

reflect the renormalization of the hopping term. The square-root terms ensure that the original bandwidth is obtained in the independent-particle limit. We adopt the saddle-point approximation, where the boson operators are considered to be independent of space and time.

The results for the total energy as a function of x are given in the inset of Fig. 2. For this calculation the parameter Δ_{e_g} decreases linearly from 1.3 to 0.7 eV as x goes from 0 to 1, in agreement with the expected trend. This results in t_{eff} increasing from 0.31 to 0.44 and U_{eff} decreasing from 1.33 to 1.06 eV as x goes from 0 to 1. The parameters are given for $x=0.0$,, 0.5, and 1.0 in Table I. Note, that U_{eff} is of the order of the charge-transfer energy Δ_{e_g} and much smaller than U_{dd} the Coulomb interaction between the $3d$ electrons.

The behavior of the total energy can be understood by considering the limiting cases of U_{eff} equal 0 and ∞. For $U_{\mathrm{eff}}=0$ the kinetic energy decreases monatonically on going from x equal 1 to 0. Furthermore, as x goes from 1 to 0 the differences between the kinetic energies for different dimen-

TABLE I. The model parameters used to calculate the effective parameters are $(pd\sigma)$ and Δ_{e_g} and $U_{dd}=5$ eV. For the calculation of Fig. 3 we have used $\Delta_{t_{2g}}=\Delta_{e_g}+1.1$ and $(pd\pi)=-0.45(pd\sigma)$. Δ_{e_g} is assumed to decrease linearly from $x=0$ to $x=1$. The resulting effective parameters $t_{\rm eff}$, $U_{\rm eff}$, and $\Delta E_{\rm spin}$ are given for $x=0.0$, 0.5, and 1.0. All energies are in eV.

x	0.0	0.5	1.0
(pds)	0.5	0.5	0.5
Δ_{e_g}	1.3	1.0	0.7
$t_{\rm eff}$	0.31	0.37	0.44
$U_{\rm eff}$	1.33	1.19	1.06
$\Delta E_{\rm spin}$	0.041	0.047	0.054

sions monatonically increase. For $U_{\rm eff}\rightarrow\infty$ the total energy is zero for $x=0$ (half filling), since the effective bandwidth renormalizes to zero; the minimum of the total energy curve is therefore close to $x=0.5$. For $U_{\rm eff}$ increasing from 0 to ∞ one finds that the total energy at $x=0$ approaches zero and that the minimum of the total energy curve moves from x equal 0 to 0.5. Since $U_{\rm eff}/W$, where W is the bandwidth, increases for lower dimensions, the total energy curve is closer to the $U_{\rm eff}\rightarrow\infty$ limit for lower dimensions.

The lowest kinetic energy of the e_g electrons is obtained for a ferromagnetic alignment of the core spins. However, in addition to that there is also an antiferromagnetic superexchange coupling between the core spins. The t_{2g} electrons form effective core spins with $S_{\rm core}=3/2$. The t_{2g} superexchange is related to the energy needed to flip two core spins, i.e., $\Delta E_{\rm spin}=E(S_{\rm total}=3)-E(S_{\rm total}=0)$. Figure 2 shows the magnetic structures with the lowest energy as a function of doping x and $\Delta E_{\rm spin}$. When increasing the superexchange between the t_{2g} spins the antiferromagnetic structures become stabilized with respect to the ferromagnetic structure, as shown in Fig. 2. Therefore, for large values of $\Delta E_{\rm spin}$ the system becomes purely antiferromagnetic, i.e., G type. First, we should point out that we do not obtain the correct magnetic structure (A type) at $x=0$. This is most likely due to our assumption of undistorted MnO_6 octahedra. The presence of Jahn-Teller effects leads to a $3x^2-r^2$; $3y^2-r^2$ orbital ordering that is crucial in obtaining the right magnetic structure for $x=0$.[17,18] In order to obtain an estimate of $\Delta E_{\rm spin}$, we performed a calculation for a Mn-O-Mn cluster with three t_{2g} electrons per Mn ion. The model parameters for the t_{2g} electrons differ from those of the e_g electrons. In this calculation we used the phenemenological relation between the tight-binding parameters $(pd\pi)=-0.45(pd\sigma)$ (Ref. 19) and a charge-transfer energy of $\Delta_{t_{2g}}=\Delta_{e_g}+1.1$ eV. The larger value of $\Delta_{t_{2g}}$ compared to Δ_{e_g} results from the higher energy of the $t^3_{2g\uparrow}t_{2g\downarrow}\underline{L}$ with respect to the $t^3_{2g\uparrow}e_{g\uparrow}\underline{L}$ configuration, due to the Hund's coupling. Throughout the series we have $\Delta_{t_{2g}}=2.4-1.8$ eV giving $\Delta E_{\rm spin}\cong 41-54$ meV; this increase should be compared with experiment, where one finds that the exchange coupling for $CaMnO_3$ is ~ 1.4 times the interplanar antiferromagnetic coupling for $LaMnO_3$.[21]

From Fig. 2 we find, for $\Delta E_{\rm spin}\cong 0.04-0.06$ eV, a number of features that are in good agreement with experiment. Most notably, the magnetic phase diagram is strongly asymmetric as a function of doping.[2,3] For $x<0.5$ one finds ferromagnetism and for $x>0.5$ different antiferromagnetic structures are observed. In the latter region we have mainly the C type structure. From neutron diffraction Wollan and Koehler[2] have established here the presence of C and CE type structures, i.e., structures with chainlike ferromagnetic regions. C type structures are relatively stable in the region $x>0.5$ since, in the independent particle limit, the bands are filled in such a way that the double occupancy is zero, since one of the two bands is nondispersive (if the ferromagnetic chain is along the z axis this band is formed by the x^2-y^2 orbitals that have a zero hybridization matrix element in the z direction).

Therefore, when increasing $U_{\rm eff}$, the total energies of the two and three dimensional structures are renormalized whereas the one dimensional system remains unaffected for $x>0.5$. When approaching $x=1$ we obtain the G type structure, as observed experimentally. Furthermore, close to $x=0.5$ several types of magnetic structures are present. This region is very sensitive to lattice deformations and it is essential to include these in order to obtain the right magnetic structure, as we show below.

We emphasize that the inclusion of states with both e_g orbitals occupied is essential for the asymmetry of the phase diagram with respect to $x=0.5$. Increasing $U_{\rm eff}$ would suppress charge fluctuations of the type $e_{g\uparrow};e_{g\uparrow}\leftrightarrow e^2_{g\uparrow};e^0_{g\uparrow}$, thereby reducing the ferromagnetic coupling between the e_g electrons. Inclusion of a finite $U_{\rm eff}$, but neglect of the degeneracy of the e_g orbitals,[7] would give rise to antiferromagnetic interactions, which does not correspond to the expected magnetic coupling between the e_g spins.

The two dominant structural changes are variations of the Mn-O-Mn bond angles and Jahn-Teller distortions. The former is a result of different ionic radii of the ions on the A site. For smaller ions the MnO_6 octahedra rotate to reduce the space around the A ion, causing a decrease in the Mn-O-Mn bond angle. Although the distance between the Mn ions becomes smaller a reduction in the effective hopping $t_{\rm eff}$ is found. For the undistorted lattice the coupling between the two Mn ions via the oxygen results from pure σ bonding. Away from 180° the bonding becomes partly σ and partly π. Since $(pd\pi)$ is about half $(pd\sigma)$ a reduction of $t_{\rm eff}$ is found. For the superexchange between the t_{2g} spins the opposite trend is found. For 180° the bonding between the t_{2g} and oxygen is π like; reducing the angle introduces a significant amount of σ bonding, leading to an increase in $\Delta E_{\rm spin}$.

Hwang *et al.*[8] find, for $x=0.3$, that a reduction of the bond angle [which they relate to the tolerance factor $d_{\rm A\text{-}O}/(\sqrt{2}d_{\rm Mn\text{-}O})$] leads to canting of the moments. A calculation at $x=0.3$ for the Mn-O-Mn cluster gives an increase in the ratio $\Delta E_{\rm spin}/t_{\rm eff}$ by a factor 1.5 when reducing the bond angle from 180° to 160°. This implies that a reduction of the tolerance factor should be interpreted as moving upwards, at a fixed doping level, in the phase diagram of Fig. 2. For $x=0.3$, one approaches the transition from the F to the A type structure. It is natural to assume that, in a model where the t_{2g} spins are not fixed along one particular axis, this transition occurs through a gradual canting of the spins between neighboring ac planes.[6]

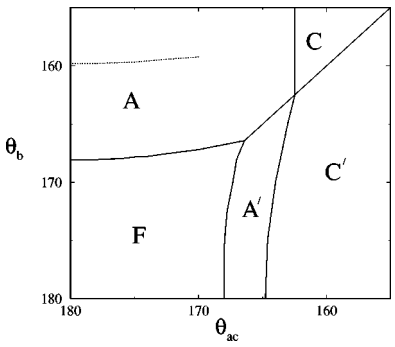

FIG. 3. The lowest magnetic structure for $x=0.5$ as a function of the Mn-O-Mn bond angle in the ac plane and along the b direction. The dotted line shows the effect of switching on a crystal field of 0.15 eV; see text.

Effects of the crystal structure on magnetic and transport properties are even more pronounced close to $x=0.5$.[9,10] Figure 3 shows the effect of changes in the Mn-O-Mn bond angle in the ac plane and along the b direction on the phase diagram. The parameters are given in Table I. Although the competition between the low-temperature magnetic structures depends mainly on the Mn-O-Mn bond angles, further changes in the boundaries between the different magnetic phases could occur as a result of different Mn-O distances and variations in parameters $[\Delta_{e_g},\Delta_{t_{2g}},(pd\sigma)]$ for different compounds.

For 180° bond angles the system is ferromagnetic. This is close to the situation found for $La_{1/2}Sr_{1/2}MnO_3$. When decreasing θ_b, the superexchange along the b direction increases while $t_{\rm eff}$ decreases. Clearly this stabilizes the A structure with respect to the ferromagnetic one. On the other hand, a reduction of the angle in the plane θ_{ac} leads to the formation of a ferromagnetic plane perpendicular to the ac plane. In both cases the largest bond angles lie in the ferromagnetic plane. A and A' are also observed experimentally close to $x=0.5$. $Nd_{0.45}Sr_{0.55}MnO_3$ has $\theta_b=162°$ and $\theta_{ac}=168°$ and is ferromagnetic in the ac plane. $Pr_{1/2}Sr_{1/2}MnO_3$ has $\theta_b\cong 174°$ and $\theta_{ac}\cong 163°$; here Kawano *et al.*[9] find ferromagnetic planes perpendicular to the ac plane. Earlier studies,[20] however, showed the chainlike CE structure. We find that the angles are close to the boundary between the planar (A') and chainlike (C') structures. When decreasing the Mn-O-Mn angles further, it becomes advantageous to increase the number of antiferromagnetic bonds, thereby forming the C and C' structures. Experimentally the chainlike CE structure is observed for $Nd_{1/2}Sr_{1/2}MnO_3$ (Ref. 9) ($\theta_b\cong\theta_{ac}=162°$) and $La_{1/2}Ca_{1/2}MnO_3$ (Ref. 10) ($\theta_b=160°$ and $\theta_{ac}=162°$).

For the comparison of high and low-temperature magnetic phases one has to consider not only changes in the Mn-O-Mn bond angle, but also the Jahn-Teller distortions. Ferromagnetic $Pr_{1/2}Sr_{1/2}MnO_3$ has bond angles $\theta_b=158°$ and $\theta_{ac}=171°$. According to Fig. 3 this would imply an A type structure. However, in this compound the MnO_6 octahedra are elongated along the b direction, thereby lowering the energy of the $3z^2$-r^2 orbital with respect to the x^2-y^2. However, the $3z^2$-r^2 orbital hybridizes less in the ac plane as compared to the x^2-y^2 orbital thereby making the A structure less favorable. The dotted line in Fig. 3 shows the change in the boundary between the F and A type structures for $\theta_{ac}\geqslant 170°$ as a result of the Jahn-Teller distortion. We used here a splitting of the effective e_g orbitals in Eq. (1) of 0.15 eV, a value that should be compared with that for the crystal field between the e_g and t_{2g} of 0.7–1.0 eV.

$Nd_{1-x}Sr_xMnO_3$, on the other hand, has, for x close to 0.5, a Jahn-Teller distortion at low temperatures with the Mn-O bond lengths along the b direction smaller than those in the ac plane. This stabilizes the antiferromagnetic structures with ferromagnetic regions in the ac plane, i.e., yielding the A and C structures found in these systems. Thus the antiferromagnetic structures for the Nd-compounds are stabilized by both the bond angles and the Jahn-Teller distortion. When the Jahn-Teller distortion disappears, the ferromagnetic state becomes more favorable than the antiferromagnetic structures. Also the increasing resistivity for the F, A, and C (CE) structures can be qualitatively understood from the relatively larger $U_{\rm eff}/W$ in the systems with lower dimensional ferromagnetic regions and the smaller $t_{\rm eff}$. Within a model that includes dynamic Jahn-Teller distortions[18] these effects lead to a crossover from a Fermi liquid to a polaronic regime.[22]

To summarize, we have interpreted the appearance of different magnetic structures as a competition between ferromagnetic regions of different dimensions and the superexchange of the t_{2g} spins. The inclusion of a finite $U_{\rm eff}$ explains the large ferromagnetic region for $x<0.5$ and the antiferromagnetic regions for $x>0.5$. This implies that, not only the double exchange mechanism $(t^3_{2g\uparrow}e_{g\uparrow};t^3_{2g\uparrow}\leftrightarrow t^3_{2g\uparrow};t^3_{2g\uparrow}e_{g\uparrow})$, but also transfer processes of the type $(t^3_{2g\uparrow}e_{g\uparrow};t^3_{2g\uparrow}e_{g\uparrow}\leftrightarrow t^3_{2g\uparrow};t^3_{2g\uparrow}e^2_{g\uparrow})$ are important for the stabilization of ferromagnetism.

Using this model we are able to elucidate the changes in magnetic structure close to x equal 0.5 and effects resulting from changes in the tolerance factor. We can therefore conclude that the present model provides a good understanding of the observed trends in the competition between different magnetic structures.

We acknowledge D. Koelling and M. R. Norman for a careful reading of the manuscript. This work has been supported by DARPA/ONR, the State of Illinois under HECA, and by U.S. DOE BES-MS under Contract No. W-31-109-ENG-38.

[1] G. H. Jonker and J. H. van Santen, Physica (Amsterdam) **16**, 337 (1950); R. von Helmolt, J. Wecker, B. Holzapfel, L. Schultz, and K. Samwer, Phys. Rev. Lett. **71**, 2331 (1993).

[2] E. O. Wollan and W. C. Koehler, Phys. Rev. **100**, 545 (1955).

[3] P. E. Schiffer, A. P. Ramirez, W. Bao, and S.-W. Cheong, Phys. Rev. Lett. **75**, 3336 (1995).

[4] C. Zener, Phys. Rev. **82**, 403 (1951).

[5] P. W. Anderson and H. Hasegawa, Phys. Rev. **100**, 675 (1955).

[6] P.-G. de Gennes, Phys. Rev. **118**, 141 (1960).
[7] J. Inoue and S. Maekawa, Phys. Rev. Lett. **74**, 3407 (1995).
[8] H. Y. Hwang, S.-W. Cheong, P. G. Radaelli, M. Marezio, and B. Batlogg, Phys. Rev. Lett. **75**, 914 (1995).
[9] H. Kawano, R. Kajimoto, H. Yoshizawa, Y. Tomoika, H. Kuwahara, and Y. Tokura, Phys. Rev. Lett. **78**, 4253 (1997).
[10] P. G. Radaelli, D. E. Cox, M. Marezio, S.-W. Cheong, P. E. Schiffer, and A. P. Ramirez, Phys. Rev. Lett. **75**, 4488 (1995).
[11] J.-H. Park, C.-T. Chen, S.-W. Cheong, W. Bao, G. Meigs, V. Chakarain, and Y. U. Idzerda, Phys. Rev. Lett. **76**, 4215 (1996).
[12] H. L. Ju, H.-C. Sohn, and K. M. Krishnan, Phys. Rev. Lett. **79**, 3230 (1997).
[13] J. Zaanen, G. A. Sawatzky, and J. W. Allen, Phys. Rev. Lett. **55**, 418 (1985).
[14] For model calculations see, e.g., J. Zaanen and G. A. Sawatzky, Can. J. Phys. **65**, 1262 (1987).
[15] J. C. Slater and G. F. Koster, Phys. Rev. **94**, 1498 (1954).
[16] G. Kotliar and A. Ruckenstein, Phys. Rev. Lett. **57**, 1362 (1986).
[17] I. Solovyev, N. Hamada, and K. Terakura, Phys. Rev. Lett. **76**, 4825 (1996).
[18] A. J. Millis, Phys. Rev. B **55**, 6405 (1997); A. Hirota and Y. Endoh (unpublished).
[19] L. F. Mattheiss, Phys. Rev. B **5**, 290 (1972).
[20] K. Knizek, Z. Jirak, E. Pollert, F. Zounova, and S. Vratislav, J. Solid State Chem. **100**, 292 (1992).
[21] A. J. Millis, B. I. Shraiman, and R. Mueller, Phys. Rev. Lett. **77**, 175 (1996).
[22] M. van Veenendaal and A. J. Fedro (unpublished).